

# Asymptotic Expansions and Amplification of Gravitational Lens Near the Fold Caustic

A.N. Alexandrov<sup>1</sup> <sup>★</sup> and V. I. Zhdanov<sup>1,2</sup> <sup>†</sup>

<sup>1</sup> *Astronomical Observatory, National Taras Shevchenko University of Kyiv, 3 Observatorna str., Kiev 04053, Ukraine*

<sup>2</sup> *National Technical University of Ukraine “Kyiv Polytechnic Institute”, Kiev 03056, Ukraine*

Accepted – Received –; in original form –

## ABSTRACT

We present two methods that enable us to obtain approximate solutions of the lens equation near the fold caustic with an arbitrary degree of accuracy. We obtain “post-linear” corrections to the well known linear caustic approximation formula for the total amplification of two critical images of a point source. In order to obtain the non-trivial corrections we had to take into account the Taylor expansion of the lens equation near caustic up to the fourth order. The result is used to obtain amplification of the extended Gaussian source in this “post-linear” order; the amplification is reduced to the form containing three additional fitting parameters. The conditions of neglecting the correction terms are analyzed. The modified amplification formula is applied to the fitting of light curves of the Q2237+0305 gravitational lens system in the vicinity of high amplification events (HAE). We show that introduction of some of the “post-linear” corrections reduces  $\chi^2$  by 30 per cent in case of known HAE on the light curve of the image C (1999). These corrections may be important for a precise comparison of different source models on account of observational data.

**Key words:** gravitational lensing: micro – quasars: individual (Q2237+0305) – gravitational lensing: strong – methods: analytical

## INTRODUCTION

In the extragalactic gravitational lens system (GLS) there are several images of the same quasar. The light from the quasar corresponding to different images intersects the lensing galaxy in different regions. The variations of gravitational fields in these regions due to stellar motions are practically independent leading to independent brightness variations in different images (gravitational microlensing). Comparison of the light curves of different images allows one to obtain a valuable information about the lens itself and about the source as well (Schneider, Ehlers & Falco 1992; Wambsganss 2006). One of the important applications of this effect deals with a unique possibility to study a fine structure of the central quasar region in an extragalactic gravitational lens systems (GLS). This idea first proposed by Grieger, Kayser & Refsdal (1988) appeals to the high amplification events (HAE’s) in one of the images of the quasar in GLS. The conventional explanation of HAE relates it to the caustic field in the source plane formed due to the inhomogeneous gravitational field of the lensing galaxy on the line of sight of the image (Schneider et al. 1992). The source crossing of a caustic leads to a considerable brightness enhancement of the image, crossing of the fold being most probable. The corresponding brightness variations in the neighbourhood of HAE may be described approximately by a formula containing a few fitting parameters. This makes possible estimations of certain HAE characteristics, in particular, the source size (Grieger et al. 1988). For example, in case of well known GLS Q2237+0305 (Einstein Cross) several HAE was observed (Wozniak et al. 2000; Alcalde et al. 2002; Udalski et al. 2006) and the estimates of the source size have been obtained within different source models (Wyithe, Webster & Turner 1999, 2000; Wyithe et al. 2000; Yonehara 2001; Shalyapin 2001; Shalyapin et al. 2002; Bogdanov & Cherepashchuk 2002). Almost all of HAE in GLS

<sup>★</sup> E-mail: alex@observ.univ.kiev.ua

<sup>†</sup> E-mail: ValeryZhdanov@mail.ru

Q2237+0305 are attributed just to the fold caustic crossing in the source plane (e.g., Gil-Merino et al. 2006). A possibility to distinguish different source models is also discussed (see, e.g., Goicoechea et al. 2003).

The lens equation near a fold may be expanded in powers of local coordinates; in the lowest orders of this expansion the caustic is represented by a straight line; so this approximation is often referred to as “linear caustic approximation”. In this approximation the point source flux amplification is given by a simple formula, which depends on the distance to the caustic and contains two parameters (see, e.g., Schneider et al. 1992). In most cases the linear caustic approximation is sufficient to fit the observed light curves over the range of HAE at modern accuracy of the flux measurement. The need for a modification of this formula (e.g., by taking into account the caustic curvature) is nevertheless being discussed for a long time (Fluke&Webster 1999; Shalyapin 2001). One may hope that future improvement of the photometric accuracy will make it possible to obtain additional parameters of the lens mapping, which are connected to the mass distribution in the lensing galaxy. At the same time in this paper we show that taking into consideration of “post-linear” terms is sometimes appropriate even to explain the present observational data. Note also that the corrections to the amplification coefficient at macrolensing were the subject of investigations in connection with the problem of “anomalous flux ratios” (Keeton, Gaudi & Petters 2005).

We note that since the work by Kochanek (2004) followed by a number of authors (Mortonson, Schechter & Wambsganss 2005; Gil-Merino et al. 2006; Vakulik et al. 2007; Anguita et al. 2008; Poindexter, Morgan & Kochanek 2008; Poindexter & Kochanek 2010a,b) statistical methods dealing with the complete light curves of the GLS images have been developed. This approach is very attractive because it allows to take into account the whole aggregate of observational data on image brightness variations yielding estimates of the microlens masses and source model parameters. However, this treatment involves a large number of realizations of microlensing field and it requires a considerable computer time. On the other hand, the source structure manifests itself only in the HAE; far from the caustics the source looks like the point one and all the information about its structure is being lost. If we restrict ourselves to the HAE neighbourhood, then we use the most general model concerning the microlensing field described by a small set of coefficients in the lens mapping. Therefore, less time consuming semi-analytical investigations dealing with caustic neighbourhoods still preserve their importance, not speaking about their use in computer codes.

In this paper we propose relations for the total amplification of two critical images of a point source in the first non-trivial “post-linear” approximations and use them to modify the amplification of an extended Gaussian source near the fold caustic. In order to obtain non-zero corrections to the total amplification of two critical images we had to take into consideration additional higher order terms in the expansion of the lens mapping in comparison with earlier works (see, e.g., Keeton et al. 2005). Though the corrections are expected to be small, in some cases they appear to be noticeable even in the analysis of the existing data on light curves in GLS Q2237+0305. The structure of this paper is as follows: after derivation of the approximate solutions of the lens equation in the required order we get the amplification of the point source. The result is applied to obtain the amplification of a small Gaussian source near the fold caustic. We use the formula for amplification of the extended source to fit the light curves in GLS Q2237+0305. The obtained post-linear corrections appear to improve agreement with the observational data.

## 1 INITIAL EQUATIONS

First we remind some general notions of the gravitational lensing that may be found, e.g., in the book by Schneider et al. (1992). The normalized lens equation has the form:

$$\mathbf{y} = \mathbf{x} - \nabla \Phi(\mathbf{x}), \quad (1)$$

$\Phi(\mathbf{x})$  is the lens mapping potential; this equation relates every point  $\mathbf{x} = (x_1, x_2)$  of the image plane to the point  $\mathbf{y} = (y_1, y_2)$  of the source plane. In general case there are several solutions  $\mathbf{X}_{(i)}(\mathbf{y})$  of the lens equation (1) that represent images of one point source at  $\mathbf{y}$ ; we denote solution number with the index in parentheses.

In case of no continuous matter on the line of sight the potential must be a harmonic function  $\Delta \Phi = 0$ . Below we will assume that this condition is fulfilled in the considered neighbourhood of the critical point. We note, however, if we suppose that during HAE the continuous matter density is constant, the lens equation may be represented in the form (1) by a suitable renormalization of the variables.

The amplification of a separate image of a point source is

$$K_{(i)}(\mathbf{y}) = 1 / |J(\mathbf{X}_{(i)}(\mathbf{y}))|, \quad (2)$$

where  $J(\mathbf{x}) \equiv |D(\mathbf{y})/D(\mathbf{x})|$  is the Jacobian of the lens mapping. In microlensing processes micro-images cannot be observed separately; therefore we need the total amplification, which is a sum of the amplification coefficients of all the images.

The critical curves of the lens mapping (1) are defined by equation  $J(\mathbf{x}) = 0$  and are mapped onto the caustics on the source plane. The stable critical points of two dimensional mapping may be folds and cusps only, the folds being more probable in HAE. In this paper we confine ourselves with consideration of the fold caustics. When a point source approaches

the fold caustic from its convex side, two of its images approach the critical curve and their amplification tends to infinity; they disappear after the source crossing of the caustic. These two images are called critical.

The standard consideration of the caustic crossing events deals with the Taylor expansion of the potential near some point  $p_{cr}$  of the critical curve in the image plane. Let this point be the coordinate origin and we suppose that (1) maps  $p_{cr}$  onto the coordinate origin on the source plane. Further we rotate synchronously the coordinate systems until the abscissa axis on the source plan will be tangent to the caustic at the origin,  $|y_2|$  locally defines the distance to the caustic and  $y_1$  defines a displacement along the axis. For the harmonic potential one can write

$$\begin{aligned} y_1 &= 2x_1 + a(x_1^2 - x_2^2) + 2bx_1x_2 + c(x_1^3 - 3x_1x_2^2) - d(x_2^3 - 3x_2x_1^2) + gx_2^4 + \dots, \\ y_2 &= b(x_1^2 - x_2^2) - 2ax_1x_2 + d(x_1^3 - 3x_1x_2^2) + c(x_2^3 - 3x_2x_1^2) + fx_2^4 + \dots, \end{aligned} \quad (3)$$

$a, b, c, d, g, f$  are the expansion coefficients. If the  $y_2$  axis is directed toward the convexity of the caustic, then  $b < 0$  (at fold points  $b \neq 0$ ).

## 2 EXPANSION OF THE CRITICAL SOLUTIONS IN POWERS OF A SMALL PARAMETER

### 2.1 Method 1

Now we proceed to derivation of the approximate solutions of Eqs. (3). To do this we present two different methods, they will be used to have a possibility of mutual checks of cumbersome calculations. The first method deals with analytical expansions in powers of small parameter, however it results in non-analytical functions of coordinates leading to nonintegrable terms in the amplification coefficient. The second method does not lead to such problems though it uses somewhat more complicated representation of solution of the lens equation (containing square roots of analytical functions). The methods agree with each other in a common domain of validity; moreover, we use the second method to justify some expressions in the amplification formulas in terms of distributions to validate applications to the extended source models.

First we shall use a regular procedure proposed by Alexandrov et al. (2003) in order to construct solutions of Eqs. (3) with a desired accuracy. This procedure is useful to study the light curve of the point source, which has a trajectory crossing the fold caustic under some non-zero angle. We suppose that the source and the caustic lay on different sides from  $y_1$  axis. Then for  $y_2 > 0$  we substitute

$$y_i = t^2 \tilde{y}_i, \quad x_1 = t^2 \tilde{x}_1, \quad x_2 = t \tilde{x}_2, \quad (4)$$

where  $i = 1, 2$  and  $t$  may be considered as a parameter of vicinity to the caustic. This is a formal substitution that makes easier operations with different orders of the expansion; after performing calculations we shall put  $t = 1$  and thus return to initial variables  $y_i$ . However, if we put  $\tilde{y}_i$  to be constant with varying  $t$ , then this substitution allows to study a local behaviour of critical image trajectories;  $t = 0$  corresponds to point source caustic crossing and  $t^2$  may be considered as the time counted from the moment when two critical images appear. This interpretation may be justified: one can show (Alexandrov et al. 2003) that two critical solutions  $\mathbf{X}_i(t) = (X_{(i)1}, X_{(i)2})$  of the lens equation can be represented by analytical functions of  $t$  that in the above special coordinate system indeed have the behaviour:  $X_{(i)1} \sim O(t^2)$ ,  $X_{(i)2} \sim O(t)$  (see Appendix A). This allows us to look for the solutions of Eqs. (3) using the expansions of  $\tilde{x}_i$  in powers of  $t$ :

$$\begin{aligned} \tilde{x}_1 &= \tilde{x}_{10} + \tilde{x}_{11}t + \tilde{x}_{12}t^2 + \dots, \\ \tilde{x}_2 &= \tilde{x}_{20} + \tilde{x}_{21}t + \tilde{x}_{22}t^2 + \dots. \end{aligned} \quad (5)$$

It should be stressed that analyticity in  $t$  does not mean that the coefficients of expansions (5) will be analytical functions of coordinates  $\tilde{y}_i$  in the source plane (see below).

In terms of new variables (4) system (3) takes on the form (up to the terms  $\sim t^2$ )

$$\begin{aligned} \tilde{y}_1 &= 2\tilde{x}_1 - a\tilde{x}_2^2 + t(2b\tilde{x}_1\tilde{x}_2 - d\tilde{x}_2^3) + t^2(a\tilde{x}_1^2 - 3c\tilde{x}_1\tilde{x}_2^2 + g\tilde{x}_2^4), \\ \tilde{y}_2 &= -b\tilde{x}_2^2 + t(-2a\tilde{x}_1\tilde{x}_2 + c\tilde{x}_2^3) + t^2(b\tilde{x}_1^2 - 3d\tilde{x}_1\tilde{x}_2^2 + f\tilde{x}_2^4). \end{aligned} \quad (6)$$

Substitution of expansions (5) into (6) allows to determine all the coefficients in sequence. The results of calculations are as follows.

For zero order terms:

$$\tilde{x}_{10} = \frac{1}{2} \left( \tilde{y}_1 - \frac{a}{b} \tilde{y}_2 \right), \quad \tilde{x}_{20} = \varepsilon \sqrt{\tilde{y}_2 / |b|}, \quad (7)$$

where  $\varepsilon = \pm 1$  determines two different solutions.

The first order terms are

$$\tilde{x}_{11} = -\varepsilon \sqrt{\frac{\tilde{y}_2}{|b|}} \frac{(ac - aR^2 + bd)\tilde{y}_2 + bR^2\tilde{y}_1}{2b^2}, \quad \tilde{x}_{21} = \frac{1}{2} \left( \frac{a^2 - c}{b^2} \tilde{y}_2 - \frac{a}{b} \tilde{y}_1 \right), \quad (8)$$

where  $R^2 = a^2 + b^2$ . The solutions up to this accuracy has been obtained earlier by Alexandrov et al. (2003) and Keeton et al. (2005). The contributions of this order are cancelled in calculations of the total amplification coefficient of two critical images. Therefore to obtain a non-trivial correction to zero order amplification we need the higher order approximations.

The second order terms contain non-analytical in  $\tilde{y}_2$  expressions:

$$\begin{aligned} \tilde{x}_{12} = & \frac{1}{4b^4} (3a^5 + 5a^3b^2 + 2ab^4 - 2b^3d - 2b^2g + 3ac^2 - 6a^3c + 3bcd - 8a^2bd + 2abf) \tilde{y}_2^2 + \\ & + \frac{1}{2b^3} (2a^2c - b^2c + 3abd - 2a^2R^2 - b^2R^2) \tilde{y}_1 \tilde{y}_2 + \frac{aR^2}{4b^2} \tilde{y}_1^2, \end{aligned} \quad (9)$$

$$\tilde{x}_{22} = \varepsilon \sqrt{\frac{\tilde{y}_2}{|b|}} \left[ \frac{1}{8b^3} (10a^2c - 5c^2 - 5a^2R^2 + 10abd - 4bf) \tilde{y}_2 - \frac{3}{4b^2} (ac + bd - aR^2) \tilde{y}_1 - \frac{R^2}{8b} \frac{\tilde{y}_1^2}{\tilde{y}_2} \right]. \quad (10)$$

## 2.2 Method 2

The second approach to constructing approximate solutions of the lens equation in the vicinity of the folds is described in Appendix B. This allows us to provide the critical solutions of system (3) (after substitution (4)) in the following form:

$$\tilde{x}_1 = p + tr\varepsilon\sqrt{w}, \quad \tilde{x}_2 = t\bar{s} + \varepsilon\sqrt{w}, \quad \varepsilon = \pm 1. \quad (11)$$

An iterative procedure described in Appendix B yields analytical expansions for functions  $p, r, \bar{s}, w$  both in powers of  $t$  and in powers of  $\tilde{y}_i$ . Application of this method to system (6) gives (up to the terms  $\sim t^2$ )

$$p = \tilde{x}_{10} + t^2 \tilde{x}_{12}, \quad (12)$$

where  $\tilde{x}_{10}$  and  $\tilde{x}_{12}$  are given by relations (7) and (9);

$$r = -\frac{R^2\tilde{y}_1}{2b} + \frac{\tilde{y}_2}{2b^2} [aR^2 - (ac + bd)], \quad \bar{s} = -\frac{a}{2b} \tilde{y}_1 + \frac{a^2 - c}{2b^2} \tilde{y}_2, \quad (13)$$

$$w = -\frac{\tilde{y}_2}{b} + \frac{t^2}{4b^2} \left[ R^2\tilde{y}_1^2 + \frac{6}{b} (bd - ab^2 + ac - a^3) \tilde{y}_1 \tilde{y}_2 + \frac{1}{b^2} (5a^2(R^2 - 2c) + 5c^2 - 10abd + 4bf) \tilde{y}_2^2 \right]. \quad (14)$$

As we see, all these expressions are analytical as functions of  $t$  and  $\tilde{y}_i$  both. If we expand  $\sqrt{w}$  in powers of  $t$ , then we immediately have the solution in the form (5) with the coefficients (7), (8), (9), (10).

## 3 AMPLIFICATION COEFFICIENT

### 3.1 Point source

For Jacobians  $J(\mathbf{X}_{(i)}(t^2\tilde{y}))$  ( $i = 1, 2$  corresponds to  $\varepsilon = \pm 1$ ) we obtain up to the terms  $\sim t^3$ :

$$\begin{aligned} J = & 4\varepsilon t \sqrt{|b|\tilde{y}_2} + 4t^2 \frac{(R^2 - c)}{b} \tilde{y}_2 + \varepsilon t^3 \sqrt{|b|\tilde{y}_2} \left[ -3 \frac{a(R^2 - c) - bd}{b^2} \tilde{y}_1 + \right. \\ & \left. + \frac{1}{2b^3} (7a^2R^2 - 8cR^2 + 7c^2 - 6a^2c - 30abd + 24b^2c + 12bf) \tilde{y}_2 - \frac{R^2}{2b} \frac{\tilde{y}_1^2}{\tilde{y}_2} \right]. \end{aligned} \quad (15)$$

According to (2) the value  $J^{-1}$  yields the amplification of individual images. Note that the terms up to order  $\sim t^2$  were obtained by Keeton et al. (2005). The final result for the total amplification of two critical images (in terms of the initial variables  $y_i$  after putting  $t = 1$ ) is:

$$K_{cr} = \frac{1}{2} \frac{\Theta(y_2)}{\sqrt{|b|y_2}} \left[ 1 + Py_2 + Qy_1 - \frac{\kappa}{4} \frac{y_1^2}{y_2} \right], \quad (16)$$

where

$$P = 2\kappa + \frac{15}{8|b|^3} [a^2b^2 + (a^2 - c)^2] - \frac{3}{4b^2} (2f - 5ad), \quad Q = \frac{3}{4b^2} (a^3 - ac + ab^2 - bd), \quad \kappa = \frac{a^2 + b^2}{2|b|}, \quad (17)$$

$\Theta(y_2)$  is the Heaviside step function. Note that  $\kappa$  is the caustic curvature at the origin, which enters explicitly into the amplification formula.

The formula (16) yields an effective approximation for the point source amplification near coordinate origin provided that  $y_2 > 0$  and  $y_2/y_1^2$  is not too small (see the term with  $\kappa$ ). For a fixed source position this always may be satisfied by an appropriate choice of the coordinate origin so that the source will be situated almost on the normal to tangent to the caustic.

If the source is on the caustic tangent or in the region between the caustic and the tangent, then formula (16) does not represent good approximation to the point source amplification. Nevertheless, in case of an extended source we shall see that the result (16) may be used to obtain approximations to the amplification of this source even it intersects the caustic. However, to do this we need to re-define correctly the convolution of (16) with brightness distribution.

### 3.2 Transition to extended source

The total microlensed flux from an extended source with the surface brightness  $I(\mathbf{y})$  is

$$F = \iint I(\mathbf{y}(\mathbf{x})) dx_1 dx_2 = \iint K(\mathbf{y}) I(\mathbf{y}) dy_1 dy_2, \quad (18)$$

where the point source amplification  $K(\mathbf{y}) = \sum_i K_i$  is the sum of amplifications of all images. Near a caustic one can approximate  $K(\mathbf{y}) = K_0 + K_{cr}(\mathbf{y})$ , where  $K_0$  is an amplification of all non-critical images that is supposed to be constant during HAE and  $K_{cr}$  is the amplification of the critical images.

Formula (16) contains the nonintegrable term  $\sim \Theta(y_2)(y_2)^{-3/2}$ . Therefore the question arises of how to use formula (16) in situation when the extended source intersects a caustic and some part of the source is in the zone between the tangent and the caustic. On account of Section 2.2 it is evident that the mentioned term is the result of an expansion of the root  $\sqrt{y_2 + \kappa y_1^2 t^2/2 + \dots}$  in the approximate solution (11-14). Any nonintegrable terms in  $K_{cr}$  does not arise without using of this expansion. On this account it is easy to show that in order to define  $K_{cr}$  correctly one must replace in (16) the term  $\Theta(y_2)(y_2)^{-3/2}$  with the generalized function  $(y_2)_+^{-3/2}$  (Gel'fand & Shilov 1964). We remind that the generalized function  $y_+^{-3/2}$  of the variable  $y$  is defined by the expression

$$\int y_+^{-3/2} f(y) dy = \int_0^\infty \frac{f(y) - f(0)}{y^{3/2}} dy = 2 \int_0^\infty y^{-1/2} \frac{\partial f(y)}{\partial y} dy$$

for any test function  $f(y)$ .

After this redefinition we have

$$K_{cr} = \frac{\Theta(y_2)}{2\sqrt{|b|}y_2} [1 + Py_2 + Qy_1] - \frac{\kappa}{8\sqrt{|b|}} y_1^2 (y_2)_+^{-3/2}, \quad (19)$$

and this formula may be correctly used to derive an approximate amplification of a sufficiently smooth extended source including the case when the source is crossing the caustic.

### 3.3 Extended Gaussian source

Now we use formula (19) to derive the amplification of the Gaussian source with the brightness distribution

$$I_G(\mathbf{y}, \mathbf{Y}) = \frac{1}{\pi L^2} \exp \left\{ -\frac{(\mathbf{y} - \mathbf{Y})^2}{L^2} \right\}, \quad (20)$$

where  $\mathbf{Y} = (Y_1, Y_2)$  is the centre of the source position in the source plane and the parameter  $L$  characterizes the source size.

The amplification of an extended source is defined as the ratio of the lensed flux (18) to the flux of the unlensed source  $F_0 = \iint I(\mathbf{y}) dy_1 dy_2$ , which is equal to unity in case of distribution (20). The amplification of the Gaussian source  $K_G$  is obtained by substitution of (20) and (19) into (18).

Let us denote  $s = Y_1/L$ ,  $h = Y_2/L$  and introduce the functions

$$I_k(h) = \int_0^\infty u^{k-1/2} \exp(-u^2 + 2uh) du = \frac{1}{2} \sum_{n=0}^\infty \frac{\Gamma(\frac{1}{4} + \frac{k+n}{2})}{n!} [2h]^n. \quad (21)$$

These functions may be expressed in terms of the confluent hypergeometric function  ${}_1F_1$  or the function of the parabolic cylinder  $D$ :

$$I_k(h) = \frac{1}{2} \Gamma\left(\frac{1}{4} + \frac{k}{2}\right) {}_1F_1\left(\frac{1}{4} + \frac{k}{2}, \frac{1}{2}; h^2\right) + h \Gamma\left(\frac{3}{4} + \frac{k}{2}\right) {}_1F_1\left(\frac{3}{4} + \frac{k}{2}, \frac{3}{2}; h^2\right) = 2^{-\left(\frac{k+1}{2}\right)} \Gamma\left(k + \frac{1}{2}\right) e^{\frac{h^2}{2}} D_{-(k+\frac{1}{2})}(-\sqrt{2} \cdot h). \quad (22)$$

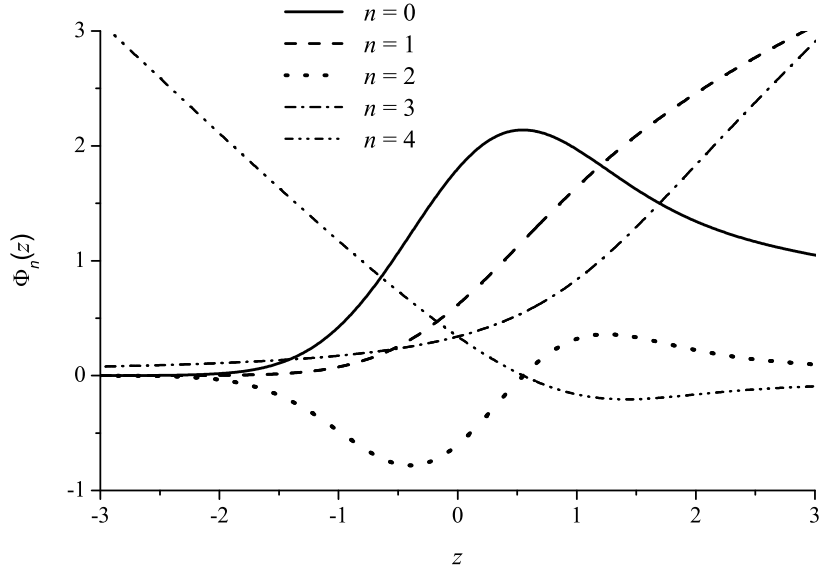


**Figure 1.** The behaviour of individual functions, which generate dependency (23), and the ratios of correction functions to the main one.

The result of calculation of (18) on account of (20) and (19) is

$$K_G(s, h) = \frac{e^{-h^2}}{2\sqrt{\pi|b|L}} \left\{ I_0(h) + L \left[ PI_1(h) - \frac{\kappa}{2} (hI_0(h) - I_1(h)) + QsI_0(h) - \kappa s^2 (hI_0(h) - I_1(h)) \right] \right\}. \quad (23)$$

We have checked this result by direct substitution of expansions (6) in the first equation (18), assuming  $t = \sqrt{L}$  and expanding the resulting integral in powers of this parameter up to the second order.

Let us discuss the formula (23) in some detail. Note that the main term of (23), which corresponds to the linear caustic approximation, was first obtained by Schneider & Weiss (1987).

To illustrate the behaviour of individual terms of Eq. (23) we introduce the following notation:

$$\begin{aligned} \Phi_0(h) &= I_0(h) \exp(-h^2), & \Phi_1(h) &= I_1(h) \exp(-h^2), & \Phi_2(h) &= [hI_0(h) - I_1(h)] \exp(-h^2), \\ \Phi_3(h) &= \Phi_1/\Phi_0, & \Phi_4(h) &= -\Phi_2/\Phi_0. \end{aligned} \quad (24)$$

These functions are shown in Fig. 1.

Note that the distinctive changes of the functions  $\Phi_0, \Phi_1, \Phi_2$  take place for  $-2L < y_2 < 2L$ . For  $y_2 < -2L$  these functions are practically equal to zero, and for  $y_2 > 2L$  they go on the asymptotic behaviour:

$$\Phi_0(h) \cong \sqrt{\frac{\pi}{h}}, \quad \Phi_1(h) \cong \sqrt{\pi h}, \quad \Phi_2(h) \cong \frac{1}{4h} \sqrt{\frac{\pi}{h}}. \quad (25)$$

The functions  $\Phi_3(h), \Phi_4(h)$  are designed to estimate the contribution of the correction terms. At the origin  $\Phi_3(0) = \Phi_4(0) = 0.338$ .

Special attention must be given to the term, which is proportional to monotonically increasing function  $\Phi_1(h)$ . This correction becomes especially noticeable on the inner side of the caustic, its sign being determined by the sign of the parameter  $P$  from Eq. (17). Such behaviour allows us to hope that the determination of this term from the observational data will not be too difficult.

The influence of the term of the formula (23) that is proportional to  $\Phi_2(h)$  is shown in Fig. 2 by the dependence  $\Phi_0(h) - \alpha\Phi_2(h)$  with different values of the coefficient  $\alpha$ . According to (23) parameter  $\alpha$  equal to half of the ratio of the source radius to curvature radius of the caustic at the origin. One can see from Fig. 2 that this term can noticeably affect the determination of the source size and the moment of caustic crossing.

The last two terms of formula (23) contain  $s \propto y_1$  and  $s^2 \propto y_1^2$ . For a fixed position of the source, one can exclude these terms by the origin displacement. In rectilinear motion of the source, the impact of these terms may be noticeable for small angles of intersection of the source trajectory with the caustic.

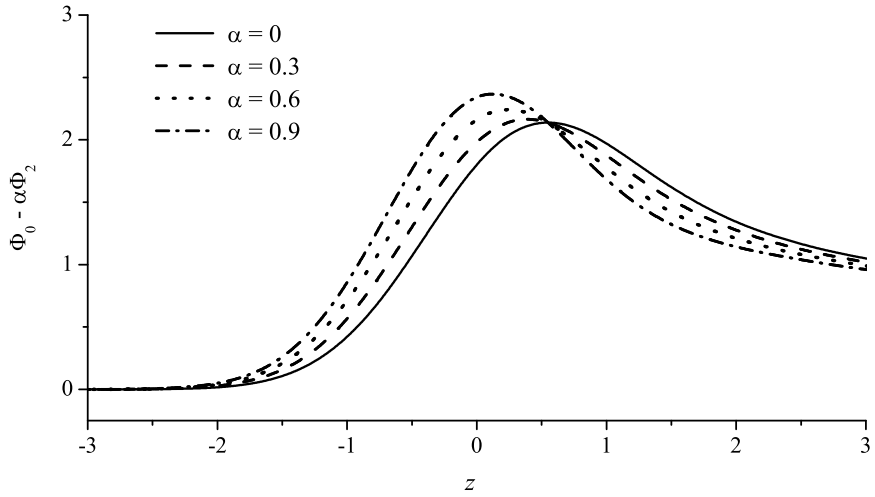


Figure 2. The influence of the correction term proportional  $\Phi_2$

We now discuss the conditions of applicability of one or another approximate formula for modelling the light curves in the vicinity of HAE. It is clear that such discussions should be based on a comparison of correction values with the accuracy of observational data. For example, let us require that in the interval  $-0.5 \leq h \leq 1$  contribution of each correction does not exceed five per cent. We see from Fig. 1 that in this range  $\Phi_3(h) < \Phi_3(1) \approx 0.83$  and  $|\Phi_4(h)| < \Phi_4(-0.5) \approx 0.73$ . From the condition of smallness of the corrections we find the following restrictions on the parameters of the model:

$$LP < 0.06, \quad L\kappa < 0.13, \quad LQ \cdot \cot(\beta) < 0.05, \quad L\kappa \cdot \cot^2(\beta) < 0.27, \quad (26)$$

where  $\beta$  is the angle between the source trajectory and the caustic. Under these conditions and within the specified margin of error one can use the linear caustic approximation. Thus, in addition to the known requirement of the smallness of the curvature of the caustic, we received a few more restrictions on the variability of the lens potential on the scale of the source size. It is clear that increasing of the requirements for the model accuracy and/or extension of the interval of  $h$  leads to strengthening of the conditions found.

Clearly, formula (23) makes sense only if we can ignore the discarded terms of higher order. This in turn means that the correction terms in (23) themselves must be sufficiently small.

#### 4 HAE IN THE EINSTEIN CROSS

The Einstein Cross QSO 2237+0305 (Huchra et al. 2008) consists of a quadruply-imaged quasar and a lensing galaxy that is the nearest of all known gravitational lens systems ( $z_G = 0.0395$ ). The gravitational delay times between images in this GLS are of the order of hours. This follows from the highly symmetric configuration of the images and partially confirmed by observations (see, e.g., Schmidt, Webster & Lewis 1998; Dai et al. 2003; Vakulik et al. 2006; Fedorova et al. 2008). Because the Einstein Cross is very suitable object for microlensing studies, its images have been continuously monitored by different groups for more than dozen of years. Significant microlensing-induced brightness peaks on light curves of the quasar images were detected in this system (see, e.g., Wozniak et al. 2000; Alcalde et al. 2002; Moreau et al. 2005).

#### Fitting the light curves and estimations of HAE parameters in GLS Q2237+0305

Now we shall apply formula (23) for fitting the light curves near HAE. For a moving source  $Y_i = V_i(t - t_C)$ , where  $t$  is the time,  $t_C$  is the moment of a caustic crossing by the source centre,  $V_i$  is the projection the source velocity on the axis  $y_i$ . We suppose that  $V_2 \gg V_1$ , i.e. the source crosses the caustic effectively and does not move along it. Our numerical simulations have shown that the terms depending upon the coordinate  $s$  contribute only for small angles between the source trajectory and the tangent to the caustic. Therefore in this paper we do not take them into account and correspondingly the parameter  $Q$  is not involved into consideration. We introduce a parameter  $T = L/|V_2|$ , then  $h = \pm(t - t_C)/T$  (the sign "+" corresponds to the source motion towards the positive direction of  $y_2$  axis).

We consider the known HAE in the light curve of image  $C$  of GLS Q2237+0305 using the OGLE data during 1999

**Table 1.** Model parameters and their central 0.95 confidence intervals as the results of light curve fitting for Q2237+0305C. The data due to OGLE group (Wozniak et al. 2000). Notation for the fitting models and parameters are given in the text.

Fitting model	$t_C$ (JD-2450000)	$T$ (days)	$A$ (mJy)	$B$ (mJy)	Correction coefficient (mJy)	$\chi^2$	$\nu$
$F^0$	$1384.7^{+1.0}_{-1.0}$	$33.0^{+2.7}_{-2.6}$	$0.364^{+0.006}_{-0.006}$	$0.076^{+0.003}_{-0.003}$		1.35	40
$F^1$	$1382.6^{+1.5}_{-1.7}$	$34.7^{+2.9}_{-2.7}$	$0.366^{+0.006}_{-0.006}$	$0.079^{+0.004}_{-0.004}$	$C = -0.006^{+0.003}_{-0.004}$	0.99	39
$F^2$	$1367.1^{+4.4}_{-3.4}$	$40.1^{+3.2}_{-3.5}$	$0.363^{+0.006}_{-0.007}$	$0.067^{+0.005}_{-0.004}$	$D = -0.071^{+0.014}_{-0.010}$	0.90	39
$F^3$	$1383.3^{+1.3}_{-1.4}$	$34.9^{+3.2}_{-2.6}$	$0.358^{+0.007}_{-0.008}$	$0.080^{+0.005}_{-0.004}$	$E = -0.004^{+0.002}_{-0.003}$	1.01	39

(Wozniak et al. 2000). Let  $F_0$  be the flux from the image  $C$  when the microlensing is absent. Under supposition that the proper brightness variations of the quasar in GLS may be neglected and taking into account the expression (23) for the magnification, we obtain the formula for fitting the flux from the microlensed Gaussian source:

$$F^M(t) = A + B\Phi_0(h) + C\Phi_1(h) + D\Phi_2(h), \quad (27)$$

which contains parameters

$$A = F_0 K_0, \quad B = F_0 \sqrt{4\pi T |b| |V_2|}, \quad C = F_0 P \sqrt{T |V_2| / 4\pi |b|}, \quad D = -\frac{1}{4} F_0 \kappa \sqrt{T |V_2| / \pi |b|}$$

that are linear, and  $t_C$  and  $T$  appearing nonlinearly. The value  $K_0$  in the expression for  $A$  is the part of the amplification due to non-critical images. The parameters  $A$  and  $B$  are evidently positive,  $D$  is negative,  $C$  may have values of both signs. As discussed above, the possibility to use a linear caustic approximation or the formula (23) is determined by the ratios of corrections coefficients to the coefficient  $B$  of zeroth approximation :  $C/B = LP$ ,  $D/B = -L\kappa/2$ .

To fit the light curve we used the minimization of weighted sum of squares:

$$S = \sum_{i=1}^N W_i [F_i - F^M(t_i)]^2, \quad (28)$$

where  $F_i$  is the result of  $i$ -th measurement,  $W_i = 1/\sigma_i^2$  is its weight that expressed through the corresponding dispersion estimate  $\sigma_i$  (Wozniak et al. 2000). The quality of fitting is often characterized by the parameter  $\chi^2 = S_{\min}/\nu$ , ( $\nu$  is the number of the degrees of freedom). The value of this parameter in optimal case must tend to unity.

We have considered as  $F^M$  the following models:

$$F^0(t) = A + B\Phi_0(h),$$

$$F^1(t) = A + B\Phi_0(h) + C\Phi_1(h),$$

$$F^2(t) = A + B\Phi_0(h) + D\Phi_2(h).$$

We also analyzed the model that takes into account both correction terms  $C\Phi_1(h) + D\Phi_2(h)$ . However, we found out that it does not allow to obtain coefficients that are both statistically significant. For comparison, we also considered the model with a correction term linear in  $h$ ; such correction may be caused by the quasar own variability, or by the influence of non-critical images (cf. Yonehara 2001):

$$F^3(t) = A + B\Phi_0(h) + Eh.$$

To choose a fitting interval in the vicinity of the light curve maximum, we used the fact that the values of fitting parameters are reasonably stable with respect to the reduction of the interval. This allowed us to find a preliminary estimate of the “background level”  $A$ . After that all the points above  $A$  have been involved in the final treatment.

The results of fitting with the different models are presented in Table 1. It contains estimates of the model parameters and their central 95 per cent confidence intervals that have been found by the Monte-Carlo simulations under supposition of the normal distribution of errors.

In all models the correction terms are statistically significant. The probability that the value of the correction coefficient is occasionally nonzero is certainly less than  $10^{-3}$  in every case. The models  $F^1$  and  $F^3$  fit the data equally well. On the other hand all three models may compete with each other on an equal footing (and probably with another effects such as due to a complicated source structure).

Note that the flux variation of the model light curve is roughly equal to 0.18 mJy, and the standard deviation of data is  $\sigma \approx 0.006$  mJy. Thus, the assumption of five percent tolerance in the vicinity of the maximum of light curve, which used in the preparation of criteria (26), is sufficiently realistic. In case of  $F^1$ -model we find  $C/B = LP \approx 0.076$ . Comparison with the first inequality in (26) indicates agreement with the statistical significance of the first correction term.

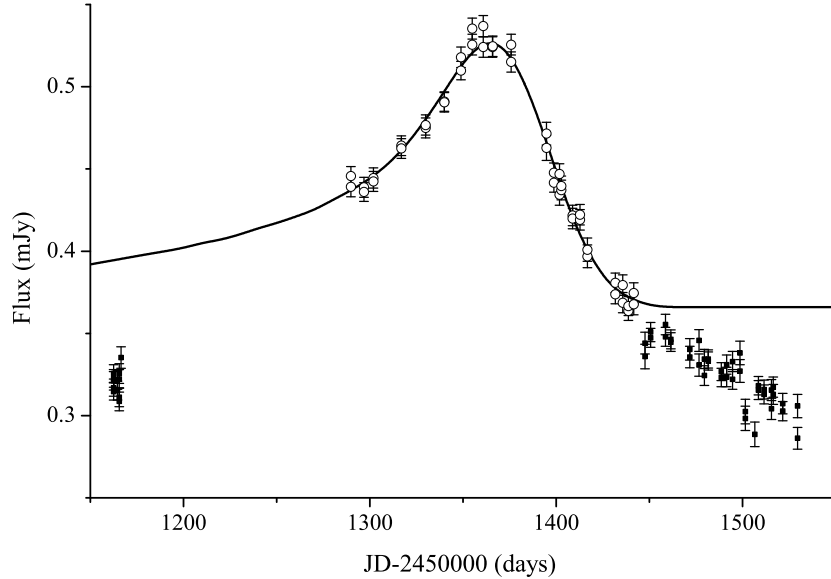


**Figure 3.** Observed light curve of Q2237+0305C (OGLE data) and the best fitting with  $F^1$  model (solid line).

Let us discuss the model  $F^2$  and role of the second correction. As compared to the other models  $F^2$  leads to somewhat lower value of  $\chi^2$ , but the confidence interval for  $t_C$  is four times wider than in case of the model  $F^0$  and the source size appears to be 20 per cent more than for other models. Here the typical features of the second correction mentioned in the previous section become apparent. True determination of  $D$  from the formula (27) could allow to estimate the ratio of curvature and source radii:  $\kappa L = -2D/B$ . But the obtained value of  $D$  corresponds to the curvature radius  $R_c \equiv 1/\kappa$  that is about twice less than the source “size”  $L$ ; so the condition of smallness of the correction is violated and the model  $F^2$  is not acceptable. On the other hand, neglecting the second correction in (27), i.e. transition to model  $F^1$ , corresponds to  $R_c \gg L$ . Our calculations have shown that a priori assignment  $R_c > L$  and the introduction of the appropriate additional term in the model  $F^1$  has little influence on estimates of  $A, B, C$ .

Fig. 3 shows the results of the light curve fitting for the image C in the region of HAE with the model  $F^1$ . Here 44 data points were included corresponding to [1289,1442] epochs interval (light circles).

To sum up, the model  $F^1$  satisfactory fits the data on HAE in question within the present accuracy, though we cannot rule out competing models and/or competing effects.

We also analyzed HAE in the light curve of image Q2237+0305A that happened in 1999 (Wozniak et al. 2000). However, the treatment of this HAE does not allowed us to find statistically significant estimates of the corrections because of lacking the data corresponding to the caustic inner region.

## 5 DISCUSSION

We proposed two methods that enable us to obtain critical solutions of the gravitational lens equations near the fold caustic. The first method is based on the expansion of the solutions and amplification coefficient  $K_{cr}$  of two critical images of the point source in powers of a formal parameter  $t$  that may be interpreted as a parameter describing proximity to the caustic. We derived a representation of  $K_{cr}$ , which is convenient to obtain amplification coefficients of extended sources. This representation is not analytical in local coordinates, and  $K_{cr}$  contains nonintegrable term. In order to elucidate these terms we considered a different representation of the solutions, which contains analytical functions of coordinates and parameter  $t$  as well as the square roots of such functions. This method yields only integrable expressions and explains the meaning of the nonintegrable term in  $K_{cr}$ : this must be considered as a generalized function, which may be used to calculate amplification of small (and smooth) extended source near the fold caustic by taking appropriate convolution.

In order to obtain non-trivial corrections to  $K_{cr}$  we had to use higher orders of expansion of the lens equation as compared to the papers by Alexandrov et al. (2003), Keeton et al. (2005). This is the consequence of cancellation of terms  $\sim O(t^2)$ , which are present in amplifications of separate critical images. Therefore we had to deal with the terms of the order  $\sim O(t^3)$  and the Taylor expansion including 4-th order in the lens equation (3). The modified formula for  $K_{cr}$  contains 3 extra

parameters that are combinations of 5 coefficients of the Taylor expansion (we confined ourselves to the case of no continuous matter on the line of sight).

On account of our result on  $K_{cr}$  we derived an asymptotic formula for amplification of the small Gaussian source  $K_G$ . We analyzed the role of the new “post-linear” corrections and formulated the conditions of applicability of the linear caustic approximation. Fitting of the light curve of GLS Q2237+0305C shows that some of these corrections may be statistically significant.

Of course, we are far from the thought that existing observational data make possible simultaneous determination of all additional parameters (and even more so the coefficients of expansion of the lens mapping up to the orders involved). Such determination require considerable improving of the photometric accuracy in future. Our aim is more modest: we show that even at the present level of accuracy some elements of the light curves may require taking into account the higher order terms in the solution of the lens equation. At least, after introduction of some post-linear corrections  $\chi^2$  decreases by 30 per cent thus approaching to 1. One may hope that enhancement of observational accuracy will increase the role of post-linear approximations.

In this connection we note that, besides estimating the source size in GLS on the basis of light curves, a number of authors (Shalyapin 2001; Shalyapin et al. 2002; Bogdanov & Cherepashchuk 2002; Goicoechea et al. 2003; Kochanek 2004; Mortonson, Schechter & Wambsganss 2005; Gil-Merino et al. 2006; Vakulik et al. 2007; Anguita et al. 2008) discuss some delicate questions concerning fine quasar structure. For example, Goicoechea et al. (2003) write that the GLITP data (Alcalde et al. 2002) on GLS Q2237+0305 admit only accretion disc models (see also Gil-Merino et al. 2006; Anguita et al. 2008). Obviously, the presence of an accretion disk in the central region of quasar is not beyond any doubts as well as the fact that the real appearance of the quasar core may be quite different from simplified models. On the other hand Mortonson, Schechter & Wambsganss (2005) argue that the accretion disk may be modelled with any brightness profile (Gaussian, uniform etc) and this model will agree with the available data provided that appropriate source size is chosen. Anyway, in these considerations different effects come into play and consistent treatment requires taking into account all the corrections to amplification including those obtained in the present paper.

## ACKNOWLEDGMENTS

This work has been supported in part by "Cosmomicrophysics" program of National Academy of Sciences of Ukraine.

## REFERENCES

Alcalde D. et al., 2002, *ApJ*, **572**, 729  
 Alexandrov A.N., Zhdanov V.I., Fedorova E.V., 2003, *Visnyk Kyivskogo Universytetu, Astronomiya* (in Ukrainian), **39-40**, 52  
 Anguita T., Schmidt R.W., Turner E.L., Wambsganss J., Webster R.L., Loomis K.A., Long D., MacMillan R., 2008, *A&A*, **480**, 327  
 Bogdanov M.B., Cherepashchuk A.M., 2002, *Astronomy Repts.*, **46**, 626  
 Dai X., Agol E., Bautz M.W., Garmire G.P., 2003, *ApJ*, **589**, 100  
 Fedorova E.V., Zhdanov V.I., Vignali C., Palumbo G.G.C., 2008, *A&A*, **490**, 989  
 Fluke C.J., Webster R.L., 1999, *MNRAS*, **302**, 68  
 Gel'fand I.M., Shilov G.E., 1964, *Generalised Functions Vol I* (New York: Academic Press)  
 Gil-Merino R., Gonzalez-Cadello J., Goicoechea L.J., Shalyapin V.N., Lewis G.F., 2006, *MNRAS*, **371**, 1478  
 Goicoechea L.J., Alcalde D., Mediavilla E., Muñoz J.A., 2003, *A&A*, **397**, 517  
 Grieger B., Kayser R., Refsdal S., 1988, *A&A*, **194**, 54  
 Huchra J., Gorenstein V., Kent S., Shapiro I., Smith G., Horine E., Perley R., 1985, *AJ*, **90**, 691  
 Keeton C.R., Gaudi B.S., Petters A.O., 2005, *ApJ*, **635**, 35  
 Kochanek C.S., 2004, *ApJ*, **605**, 58  
 Moreau O., Libbrecht C., Lee D.-W., Surdej J., 2005, *A&A*, **436**, 479  
 Mortonson M.J., Schechter P.L., Wambsganss J., 2005, *ApJ*, **628**, 594  
 Petters A.O., Levine H., Wambsganss J., 2001, *Singularity Theory and Gravitational Lensing* (Boston: Birkhäuser)  
 Poindexter S., Kochanek C.S., 2010, *ApJ*, **712**, 658  
 Poindexter S., Kochanek C.S., 2010, *ApJ*, **712**, 668  
 Poindexter S., Morgan N., Kochanek C.S., 2008, *ApJ*, **673**, 34  
 Poston T., Stewart I., 1978, *Catastrophe Theory and Its Applications* (London: Pitman)  
 Schmidt R., Webster R.L., Lewis F.G., 1998, *MNRAS*, **295**, 488  
 Schneider P., Ehlers J., Falco E.E., 1992, *Gravitational Lenses* (New York: Springer)

Schneider P., Weiss A., 1987, A&A, **171**, 49  
 Shalyapin V.N., 2001, Astronomy Lett., **27**, 150  
 Shalyapin V.N., Goicoechea L.J., Alcalde D., Mediavilla E., Muñoz J.A., Gil-Merino R., 2002, ApJ, **579**, 127  
 Udalski A., et al., 2006, Acta Astron. **56**, 293  
 Vakulik V., Schild R., Dudinov V., Nuritdinov S., Tsvetkova V., Burkhanov O., Akhunov T., A&A, **447**, 905  
 Vakulik V.G., Schild R.E., Smirnov G.V., Dudinov V.N., Tsvetkova V.S., 2007, MNRAS, **382**, 819  
 Wambsganss J., 2006, in Gravitational Lensing: Strong Weak and Micro, Saas-Fee Advanced Course 33, G. Meylan, P. North, P. Jetzer, eds., (Springer: Berlin) 453, [astro-ph/0604278]  
 Wozniak P.R., Alard C., Udalski A., Szymanski M., Kubiak M., Pietrzynski G., Zebrun K., 2000, ApJ, **529**, 88  
 Wyithe J.S., Webster R.L., Turner E.L., 1999, MNRAS, **309**, 261  
 Wyithe J.S., Webster R.L., Turner E.L., Mortlock D.J., 2000, MNRAS, **315**, 62  
 Wyithe J.S., Webster R.L., Turner E.L., 2000, MNRAS, **318**, 762  
 Yonehara A., 2001, AJ, **548**, L127

## APPENDIX A: ANALYTICAL EXPANSION METHOD

Here we present a justification of the method of analytical expansions near the folds used in the section 2.1 following Alexandrov et al. (2003). This problem is not trivial because the Jacobian of the lens mapping on the fold is equal to zero.

We say that an analytic function  $f(t)$  has order  $k$  at  $t = 0$ , if  $f^{(i)}(0) = 0$  for  $i = 0, 1, \dots, k-1$ , and  $f^{(k)}(0) \neq 0$  (Poston & Stewart 1978); then we write  $f(t) = O(t^k)$ .

It is well known that mapping

$$\mathbf{y} = \mathbf{F}(\mathbf{x}) \quad (\text{A1})$$

of two-dimensional manifolds (e.g., the mapping (3)) in the neighbourhood of the fold ( $\mathbf{x} = \mathbf{y} = 0$ ) may be reduced by coordinate transformations

$$\mathbf{u} = \mathbf{u}(\mathbf{x}), \quad \mathbf{v} = \mathbf{v}(\mathbf{y}), \quad \mathbf{x} = \mathbf{x}(\mathbf{u}), \quad \mathbf{y} = \mathbf{y}(\mathbf{v}) \quad (\text{A2})$$

to the normal form (see, e.g., Petters, Levine & Wambsganss 2001):

$$\mathbf{u} \rightarrow \mathbf{v} : \quad v_1 = u_1, \quad v_2 = (u_2)^2. \quad (\text{A3})$$

We shall suppose the initial mapping (A1) to be analytical; then the transformations (A2) are also analytical.

Let the source moves along a parameterized curve  $\mathbf{v}(t)$ , such that: (i)  $v_2(t) > 0$  for  $t \neq 0$ ,  $\mathbf{v}(0) = 0$ ; (ii) the functions  $v_i(t)$  are analytical at  $t = 0$ ; (iii) the order of  $v_2(t)$  is  $2k$  for some integer  $k \geq 1$ . The conditions (ii), (iii) mean that  $v_2(t) = t^{2k}(q + \chi(t))$ ,  $q \neq 0$ , and  $\chi(t)$  is analytical function at  $t = 0$  such that  $\chi(0) = 0$ . In view of (i) also  $q + \chi(t) > 0$ .

We have two obvious solutions of Eqs.(A3):

$$\mathbf{u}_{(\pm)}(t) = \{v_1(t), \pm t^k \sqrt{q + \chi(t)}\}, \quad (\text{A4})$$

which in view of  $q > 0$  are analytical as functions of  $t$  at the common point  $t = 0$ . We can say that the trajectory of the source consists of two branches, corresponding to values  $t < 0$  and  $t > 0$ . Each branch has two images lying on different sides of the critical curve. When  $k$  is even (odd), the images, which lie on the one hand (on different sides), analytically continued one another.

Thus a suitable choice of the source trajectory  $\mathbf{v}(t)$  leads to the analyticity of its critical images as functions of the parameter. Now we want to reformulate the sufficient conditions of the existence of the analytic solutions in the original coordinates.

The coordinate transformation  $\mathbf{y} \rightarrow \mathbf{v}$  in the source plane can be written as

$$v_1 = Ay_1 + By_2 + \Phi_1(y_1, y_2), \quad (\text{A5})$$

$$v_2 = Cy_1 + Dy_2 + \Phi_2(y_1, y_2), \quad (\text{A6})$$

$$AD - BC \neq 0.$$

Here  $\Phi_i(y_1, y_2)$  are analytical functions having Taylor expansions starting from the second order.

Next, we assume that linear in  $x_i$  terms are present only in the first component  $F_1(\mathbf{x})$  of the lens mapping (A1). Then in Eq. (A6) we have  $C = 0$ . This statement follows from substitution of (A1) into Eq. (A6) application of transformation  $\mathbf{x} = \mathbf{x}(\mathbf{u})$  and comparison with the second Eq. (A3).

Suppose that

(a) the curve  $\mathbf{y}(t)$  is lying from the inner side of the caustic (except  $\mathbf{y}(0) = 0$ ),

(b)  $\mathbf{y}(t)$  is such that  $y_1(t) = O(t^m)$ ,  $y_2(t) = O(t^{2k})$ ;  $m > k \geq 1$ ,  $m, k$  are integers.

Then from Eq.(A6) we have  $v_2(t) = O(t^{2k})$ .

In summary, we obtain the following statement.

Let the function  $\mathbf{F}(\mathbf{x})$  of the lens equation (A1) be an analytical function of  $\mathbf{x}$  in the neighbourhood of the fold critical point  $\mathbf{x} = 0$ , and  $\mathbf{y} = 0$  be the corresponding caustic point;  $F_2(\mathbf{x})$  does not contain linear terms. Let  $\mathbf{y}(t)$  be an analytical vector-function, which represents the curve satisfying conditions (a),(b).

Then the lens equation A1 has two analytical in  $t$  solutions  $\mathbf{x}_{(+)}(t)$  and  $\mathbf{x}_{(-)}(t)$  representing the critical images of the curve  $\mathbf{y}(t)$ .

These conditions are sufficient ones and they do not exhaust possible combinations of  $k, m$ . Typically the statement is true also when  $m = k$ . This statement allows us to use analytical expansions along test source trajectories to obtain the critical solutions near the folds. In the main body of this paper we have used the family of straight-line trajectories of the source  $y_i(t) = a_i t^2$  ( $k = 1, m = 2$ ) in the caustic neighbourhood on one side from the tangent to the caustic. In the paper (Alexandrov et al. 2003) we also considered the version with parabolic curves  $y_1(t) = at$ ,  $y_2(t) = bt^2$ , which allowed us to find the solutions in the approximation of parabolic caustic.

## APPENDIX B: ANALYTICAL ITERATION METHOD

In this Appendix we show that the critical solutions of the lens equation (3) (after substitution of (5)) may be represented in the form (11), the functions  $p, r, s, w$  being polynomials of  $t, y_1, y_2$  on every step of the approximation procedure.

Here we use the notations, which are independent of the rest of the paper. After a simple change of variables ( $y_1 = (b\tilde{y}_1 - a\tilde{y}_2)/2b$ ,  $y_2 = -\tilde{y}_2/b$ ) equations (6) may be written in the form

$$\begin{aligned} y_1 &= x_1 + t \sum_{n,m} a_{n,m}(t) x_1^n x_2^m, \\ y_2 &= x_2^2 + t \sum_{n,m} b_{n,m}(t) x_1^n x_2^m, \end{aligned} \quad (B1)$$

where indexes  $m, n$  take on integer non-negative finite values;  $t$  is a small parameter; the coefficients  $a_{n,m}(t), b_{n,m}(t)$  are finite order polynomials of  $t$ . In fact all considerations below may be performed in case when the r.h.s. of (B1) are analytical functions of  $x_1, x_2$  and of small parameter  $t$ . However, in this paper we deal with finite order approximations.

We look for the solution in the form

$$x_1 = p + t\varepsilon r\sqrt{w}, \quad x_2 = ts + \varepsilon\sqrt{w}; \quad \varepsilon = \pm 1. \quad (B2)$$

After substitution of (B2) into (B1) we separate the terms containing integer and half-integer powers of  $w$ , e.g.:

$$\sum_{n,m} a_{n,m}(p + \varepsilon tr\sqrt{w})^n (ts + \varepsilon\sqrt{w})^m = A_0 + \varepsilon w^{1/2} A_1,$$

where

$$A_0 = \sum_{n,m} a_{n,m} \sum_{\substack{k,k' \\ k+k'=2K}} C_n^k C_m^{k'} (tr)^k p^{n-k} (ts)^{m-k'} w^K, \quad K = \frac{k+k'}{2} \text{ is an integer,}$$

$$A_1 = \sum_{n,m} a_{n,m} \sum_{\substack{k,k' \\ k+k'=2\bar{K}+1}} C_n^k C_m^{k'} (tr)^k p^{n-k} (ts)^{m-k'} w^{\bar{K}}, \quad \bar{K} = \frac{k+k'-1}{2} \text{ is an integer.} \quad (B3)$$

Here  $C_n^k$  are the binomial coefficients,  $C_n^k = 0$  for  $k > n$  and for  $k < 0$ ;  $k, k'$  are non-negative integers.

Then we equate separately the terms with integer and half-integer powers of  $w$  in both sides of the relation following from the first equation of the system (B1) to yield

$$p = y_1 + tP(t, p, r, s, w), \quad (B4)$$

where

$$P(t, p, r, s, w) \equiv -A_0,$$

and

$$r + A_1 = 0 \quad (B5)$$

Analogously, from the second equation of (B1) we have

$$w = y_2 + tW(t, p, r, s, w), \quad (B6)$$

where

$$W(t, p, r, s, w) \equiv -ts^2 - B_0,$$

and

$$2s + B_1 = 0. \quad (B7)$$

Here  $B_0$  and  $B_1$  are defined similarly to  $A_0$  and  $A_1$  by (B3) with replacement of the coefficients  $a_{n,m} \rightarrow b_{n,m}$ .

Separating in (B3) the terms of zero order with respect to  $r, s$  (or with respect to  $t$ ) we rewrite (B5) as follows

$$r + \sum_{n,K} a_{n,2K+1} p^n w^K + tU(t, p, r, s, w) = 0, \quad (B8)$$

where

$$U(t, p, r, s, w) \equiv \sum_{n,m} a_{n,m} \sum_{\substack{k,k' \\ k+k'=2K+1 \\ k+m-k'>0}} C_n^k C_m^{k'} t^{k+m-k'-1} r^k p^{n-k} s^{m-k'} w^K.$$

Substituting  $p$  and  $w$  from (B4), (B6) into equation (B8) we get

$$r + \sum_{n,K} a_{n,2K+1} (y_1 + tP)^n (y_2 + tW)^K + tU(t, p, r, s, w) = 0.$$

This relation may be written as

$$r = f(t, y_1, y_2) + tR(t, p, r, s, w), \quad (B9)$$

where

$$f(t, y_1, y_2) \equiv - \sum_{n,K} a_{n,2K+1} y_1^n y_2^K,$$

$$R(t, p, r, s, w) \equiv - \sum_{n,K} a_{n,2K+1} \sum_{\substack{k,k' \\ k+k'=2K+1 \\ k+m-k'>0}} C_n^k C_K^{k'} y_1^{n-k} y_2^{K-k'} P^k W^{k'} t^{k+k'-1} - U(t, p, r, s, w).$$

Analogous consideration of Eq. (B7) yields

$$s + \frac{1}{2} \sum_{n,K} b_{n,2K+1} p^n w^K + \frac{t}{2} V(t, p, r, s, w) = 0,$$

where

$$V(t, p, r, s, w) \equiv \sum_{n,m} b_{n,m} \sum_{\substack{k,k' \\ k+k'=2K+1 \\ k+m-k'>0}} C_n^k C_m^{k'} t^{k+m-k'-1} r^k p^{n-k} s^{m-k'} w^K.$$

Then we substitute  $p$  and  $w$  from (B4), (B6) to obtain

$$s = g(t, y_1, y_2) + tS(t, p, r, s, w), \quad (B10)$$

where

$$g(t, y_1, y_2) \equiv - \frac{1}{2} \sum_{n,K} b_{n,2K+1} y_1^n y_2^K,$$

$$S(t, p, r, s, w) \equiv - \frac{1}{2} \left[ \sum_{n,K} b_{n,2K+1} \sum_{\substack{k,k' \\ k+k'=2K+1 \\ k+m-k'>0}} C_n^k C_K^{k'} y_1^{n-k} y_2^{K-k'} P^k W^{k'} t^{k+k'-1} + V(t, p, r, s, w) \right].$$

Thus we have a system of equations (B4), (B9), (B6), (B10) with respect to  $p, r, s, w$ , that may be represented in the form

$$\mathbf{X} = \mathbf{F}(t, \mathbf{Y}) + t \mathbf{G}(t, \mathbf{X}, \mathbf{Y}), \quad (B11)$$

where

$$\mathbf{X} = \begin{Bmatrix} p \\ r \\ s \\ w \end{Bmatrix}, \quad \mathbf{Y} = \begin{Bmatrix} y_1 \\ y_2 \end{Bmatrix}, \quad \mathbf{F}(t, \mathbf{Y}) = \begin{Bmatrix} y_1 \\ f(t, y_1, y_2) \\ g(t, y_1, y_2) \\ y_2 \end{Bmatrix}, \quad \mathbf{G}(t, \mathbf{X}, \mathbf{Y}) = \begin{Bmatrix} P(t, p, r, s, w) \\ R(t, p, r, s, w) \\ S(t, p, r, s, w) \\ W(t, p, r, s, w) \end{Bmatrix}.$$

The system (B11) is ready for iterations

$$\mathbf{X}_{(n)} = \mathbf{F}(t, \mathbf{Y}) + t \mathbf{G}(t, \mathbf{X}_{(n-1)}, \mathbf{Y}), \quad n = 1, 2, \dots, \quad \mathbf{X}_{(0)} = \mathbf{F}(t, \mathbf{Y}).$$

For a sufficiently small  $t$  the iteration process converges due to the contraction mapping theorem. It is important to note that at every iteration step we obtain an approximate solution in the form of finite order polynomials of  $\mathbf{Y}$ . This is obvious from the explicit form of the functions  $f(t, y_1, y_2)$ ,  $g(t, y_1, y_2)$ ,  $P(t, p, r, s, w)$ ,  $R(t, p, r, s, w)$ ,  $S(t, p, r, s, w)$ ,  $W(t, p, r, s, w)$ . Application of the above procedure to system (6) yields solution (11-14).

This paper has been typeset from a  $\text{\TeX}$  /  $\text{\LaTeX}$  file prepared by the author.